



Molecular rotors: synthesis and evaluation as viscosity sensors

Jeyanthi Sutharsan^a, Darcy Lichlyter^b, Nathan E. Wright^a, Marianna Dakanali^a, Mark A. Haidekker^{b,*}, Emmanuel A. Theodorakis^{a,*}

^a Department of Chemistry and Biochemistry, University of California, San Diego, 9500 Gilman Drive, La Jolla, CA 92093-0358, USA

^b Faculty of Engineering, University of Georgia, Athens, GA 30602, USA

ARTICLE INFO

Article history:

Received 20 November 2009

Received in revised form

22 January 2010

Accepted 26 January 2010

Available online 1 February 2010

ABSTRACT

It has been shown that compounds containing the *p*-*N,N*-dialkylaminobenzylidene cyanoacetate motif can serve as fluorescent non-mechanical viscosity sensors. These compounds, referred to as molecular rotors, belong to a class of fluorescent probes that are known to form twisted intramolecular charge-transfer complexes in the excited state. In this study we present the synthesis and spectroscopic characterization of these compounds as viscosity sensors. The effects of the molecular structure and electronic density of these rotors to the emission wavelength, fluorescence intensity, and viscosity sensitivity are discussed.

© 2010 Elsevier Ltd. All rights reserved.

1. Introduction

Variations in fluid viscosity are associated with a variety of functions and diseases both at the cellular¹ and organismal level.² For instance, cell membrane viscosity depends on the chemical composition of the bilayer and must have optimum values for the proper function of various membrane bound enzymes and receptors.³ Consequently, changes of membrane viscosity affect cellular signaling pathways and are associated with a variety of disorders, such as cardiovascular disease,⁴ cell malignancy,⁵ and Alzheimer's disease.⁶ In a similar fashion, changes in the viscosity of blood, plasma or lymphatic fluids have been linked to diabetes,⁷ hypertension,⁸ infarction,⁹ and aging.¹⁰

The importance of membrane viscosity in cellular biology and physiology led to the development of several methods for quantitative measurements. Among them are included mechanical methods, where the lipids and proteins are tested in a cone-and-plate viscometer or a capillary viscometer.¹¹ However, these methods are limited by the large sample size and are not effective in measuring real-time changes.¹² Alternatively, fluorescence-based methods benefit from the rapid response time and good spatial resolution of the fluorescent probes.¹³ Techniques based on fluorescence anisotropy¹⁴ (FA) and fluorescence recovery after photobleaching¹⁵ (FRAP) are commonly used in biological measurements but suffer from the need of specialized instruments, high energy light and limited spatial resolution.¹⁶ An alternative method for measuring viscosity is based on the use of a special

group of environment-sensitive fluorescent probes.¹⁷ These probes, referred to as molecular rotors, are known to form twisted intramolecular charge-transfer (TICT) complexes in the excited state producing a fluorescence quantum yield that is dependent on the surrounding environment.¹⁸ The chemical structure of the molecular rotors contains an electron donor unit in conjugation with an electron acceptor unit (D- π -A motif). Following photoexcitation, this motif has the unique ability to relax either via fluorescence emission or via an internal non-radiative molecular rotation. This internal rotation occurs around the σ -bonds that connect the electronically rich π -system with the donor and acceptor groups and can be modulated by the microenvironment of the probe.¹⁹ For instance, if such rotation is hindered due to the high viscosity of their microenvironment, the relaxation occurs via an increased fluorescence emission. In contrast, in solvents of low viscosity the relaxation proceeds mainly via a non-radiative pathway. Overall, this property results in a fluorescence emission whose quantum yield is proportional to the viscosity of the environment.

Figure 1 shows the chemical structures of two commonly used molecular rotors based on the julolidine scaffold: 9-(dicyanovinyl)-julolidine (DCVJ)²⁰ and 9-(2-carboxy-2-cyano)vinyl-julolidine

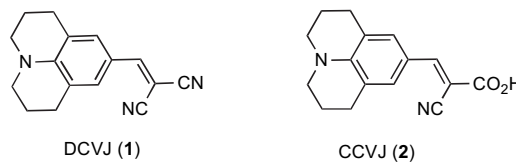


Figure 1. Representative structures of molecular rotors based on the julolidine scaffold.

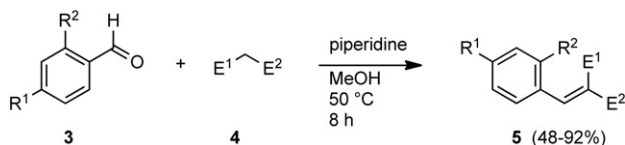
* Corresponding authors. Tel.: +1 858 822 0456; fax: +1 858 822 0386; e-mail address: etheodor@ucsd.edu.

(CCVJ).²¹ TICT formation takes place by photoinduced electron transfer from the julolidine nitrogen to one of the nitrile groups with subsequent intramolecular rotation around the julolidine–vinyl bond. Over the past years we have been exploring the applicability of molecular rotors, containing the *N,N*-dialkylaniline motif,²² as sensors for various biological and engineering applications.²³ The subject of this investigation was to evaluate whether and how changes in the chemical structure of the molecular rotors can change the emission wavelength, fluorescence intensity, and sensitivity of the viscosity measurements.

2. Results

2.1. Synthesis of molecular rotors

The synthesis of all molecular rotors was accomplished in one step by Knoevenagel condensation of 1 equiv of the appropriate aldehyde with 1.1 equiv of malonic acid derivative **4**. This reaction was catalyzed by piperidine (10%) and was completed within 8 h.²⁴ The synthesis of rotors based on the phenyl scaffold is illustrated in Scheme 1. In most cases, the desired product **5** crystallized out of methanol (Table 1).

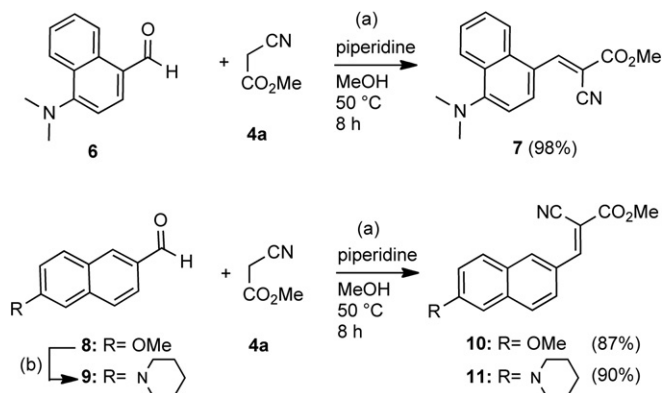


Scheme 1. Reagents and conditions: 1.0 equiv **3**, 1.1 equiv **4**, 0.1 equiv piperidine, MeOH, 50 °C, 8 h.

Table 1
Structures and yields of rotors **5a–5m**

Cmp #	R ¹	R ²	E ¹	E ²	Yield (%)
5a	OMe	H	CN	CO ₂ Me	84
5b	NH ₂	H	CN	CO ₂ Me	87
5c	NH ₂	H	CN	CN	65
5d	NMe ₂	H	CN	CO ₂ Me	89
5e	NMe ₂	H	CN	CN	91
5f	NMe ₂	H	CN	SO ₂ Ph	92
5g	NMe ₂	H	CO ₂ Me	CO ₂ Me	17
5h	NMe ₂	OMe	CN	SO ₂ Ph	81
5i	NMe ₂	OMe	CN	CO ₂ Me	89
5j	NMe ₂	Me	CN	CO ₂ Me	86
5k	NEt ₂	H	CN	CO ₂ Me	67
5l	NMe ₂	H	SO ₂ Ph	SO ₂ Ph	7
5m	NBu ₂	H	CN	CO ₂ Me	72

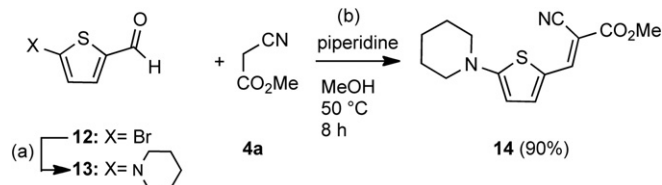
The synthesis of molecular rotors based on the naphthalene scaffold is illustrated in Scheme 2. The *p*-substituted naphthaldehyde **9** was prepared by treatment of commercially available



Scheme 2. Reagents and conditions: (a) 1.0 equiv aldehyde, 1.1 equiv α -cyanomethyl ester, 0.1 equiv piperidine, MeOH, 50 °C, 8 h; (b) 8.0 equiv piperidine, benzene/HMPA: 1:1, 0 °C, 8.0 equiv *n*-BuLi, 0 °C, 15 min, then 1.0 equiv aldehyde, 25 °C, 12 h, 35%.

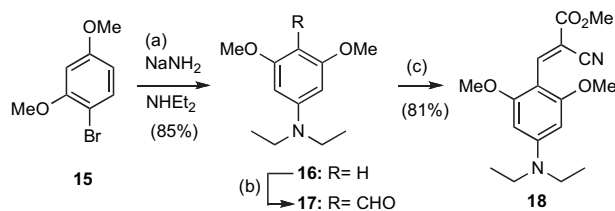
methoxy naphthaldehyde **8** with 8 equiv of lithiated piperidine.²⁵ Condensation of **6**, **8**, and **9** with methyl 2-cyanoacetate (**4a**) afforded rotors **7**, **10**, and **11**, respectively, in excellent yields.

The synthesis of molecular rotor **14**, in which the donor and acceptor groups are conjugated through a thiophene scaffold, is shown in Scheme 3. Commercially available aldehyde **12** was converted to the piperidine derivative **13** in 72% yield.²⁶ Knoevenagel condensation of **13** with **4a** produced **14** in 90% yield.



Scheme 3. Reagents and conditions: (a) 1.0 equiv aldehyde, 1.0 equiv piperidine, 0.1 equiv *p*-TsOH, toluene, 120 °C, 24 h, 72%; (b) 1.0 equiv **13**, 1.1 equiv **4a**, 0.1 equiv piperidine, MeOH, 50 °C, 8 h, 90%.

The synthesis of molecular rotor **18**, containing two methoxy groups *ortho* to the acceptor unit, is shown in Scheme 4. Treatment of 1-bromo-2,4-dimethoxybenzene (**15**) with sodium amide in the presence of diethylamine produced, via the formation of an aryne intermediate, aniline **16** in 85% yield.²⁷ Formylation of **16** under Vilsmeier conditions, followed by condensation of the resulting aldehyde **17** with **4a** produced compound **18** in 53% combined yield.²⁸



Scheme 4. Reagents and conditions: (a) 1 equiv **15**, 10 equiv NaNH₂, 75 equiv NHEt₂, 25 °C, 24 h, 85% (b) 1.0 equiv **16**, 2.0 equiv DMF, 1.1 equiv POCl₃, 2 M NaOH, 8 h, 65%; (c) 1.0 equiv aldehyde, 1.1 equiv cyanomethyl ester, 0.1 equiv piperidine, MeOH, reflux, 50 °C, 8 h, 81%.

2.2. Spectroscopic characterization of molecular rotors

In principle a good molecular rotor should have the following properties: (a) a large Stokes shift that will provide good separation between the excitation and emission light; (b) a tunable emission wavelength that can be modified as a function of the chemical structure and can be optimized for a specific application and; (c) high brightness, which translates to a high overall emission quantum yield; and (d) high sensitivity, which translates to bigger changes in emission quantum yield as a function of changes in viscosity.

As indicated above, two excited-state deactivation pathways exist for molecular rotors, the non-radiative intramolecular rotation and the fluorescent emission. The viscosity of the solvent influences the rate of the non-radiative intramolecular rotation that subsequently influences the fluorescence quantum yield.²⁹ Förster and Hoffmann found a nonlinear relationship between fluorescent quantum yield Φ_F and viscosity η as described in Eq. 1:³⁰

$$\log \Phi_F = C + x \log \eta \quad (1)$$

where x is a dye-dependent constant and C is an empirical proportionality constant. Furthermore, fluorescence emission intensity (I_F) and quantum yield (Φ_F) are proportional. With steady-state fluorescence, Eq. 1 can be reformulated as a power law Eq. 2:

$$I_F = \alpha \cdot \eta^x \quad (2)$$

where the new constant α is 10^C multiplied with predominantly instrument factors and dye concentration. The constants α and x

can be determined experimentally by measuring the peak emission intensity in solvents of different viscosities and fitting a regression line into the logarithms of the data points. Notably, α is a comparative metric for the dye's overall brightness and the slope x is a measure for the change of the intensity with viscosity, that is, the dye's viscosity sensitivity. A possible interpretation of the regression's y -intercept α is the logarithm of the emission intensity at a viscosity of 1 mPa s. We therefore use the scaled y -intercept α , given in 1000 photon counts per second, as a relative metric of brightness. Finally, the Stokes shift was calculated as the difference between emission and excitation wavelength. Table 2 summarizes these properties for the synthesized rotors.

Table 2
Fluorescent properties and viscosity profile of molecular rotors

Cmp #	Excitation λ (nm)	Emission λ (nm)	Stokes shift	Viscosity Sensitivity x	R^2	Brightness y -intercept α
1	470	503	33	0.542	>0.98	70
2	431	489	58	0.543	>0.99	147
5a^a	321	404	83	0.359	>0.99	7
5b^a	423	460	37	0.553	>0.99	50
5c^a	430	460	30	0.425	>0.99	24
5d^b	440	484	44	0.535	>0.99	85
5e	447	485	38	0.538	>0.98	61
5f	436	486	50	0.531	>0.99	146
5g	393	485	92	0.519	>0.99	17
5h	448	480	32	0.477	>0.99	295
5i^a	450	480	30	0.528	>0.99	99
5j	448	491	43	0.614	>0.99	43
5k	443	486	43	0.554	>0.99	127
5l	419	470	51	0.440	>0.99	22
5m	443	488	45	0.512	>0.99	200
7^a	466	532	66	0.521	>0.99	18
10	373	476	103	0.403	>0.98	81
11	447	598	151	0.223	>0.99	822
14	470	492	22	0.517	>0.99	112
18	433	461	28	0.562	>0.99	11

^a Average of $N=2$.

^b Average of $N=4$.

Excitation and emission spectra of selected molecular rotors are shown in Figure 2. To allow better comparison, the spectra were normalized so that the emission from the highest viscosity is unity. The dashed line represents an excitation acquisition for each derivative while solid lines are the emission spectra in different mixtures of ethylene glycol and glycerol of varying viscosity (given in mPa s). A high glycerol content increases the solvent viscosity leading to an increase in the quantum yield of the fluorescence emission.

As shown in Eq. 2, there is a power law relationship between viscosity and emission quantum yield. Figure 3 represents peak emission intensities taken from Figure 2 and drawn over viscosity in a double-logarithmic scale. The slope and the y -intercept provide the desired metrics for sensitivity and brightness.

3. Discussion

In terms of chemistry, all rotors are characterized by a small molecular weight (less than 500), a facile one- to two-step synthesis from commercially available materials and a good solubility in the solvents of interest. With the exception of the low yielding condensation reaction for the formation of **5g** and **5l**, all yields were high. Their chemical structure is defined by the presence of an electron donor group (oxygen or nitrogen) that is in conjugation with an electron acceptor group (nitrile, methyl ester of phenyl sulfone). Replacing the amino group with a weaker electron donor, such as the methoxy group,³¹ induces a blue shift to both the excitation and emission maxima in accordance to previous published results.³² This effect is manifested in both the

phenyl (Table 2, compounds **5a**, **5b**, **5d**) and naphthyl systems (Table 2, compounds **10**, **11**). Moreover, the extent of conjugation between the donor and the acceptor group influences significantly the emission wavelength and increases the Stokes shift. This effect is evident when we compare rotor **5d** (emission max=460, Stoke shift=44) with **11** (emission max=598, Stoke shift=151). On the other hand, the alkyl side chains of the nitrogen have no significant effect on the excitation and emission wavelengths (Table 2, compounds **5d**, **5k**, **5m**). Similarly, minimal changes are observed between the different acceptor groups (Table 2, compounds **5d**, **5e**, **5f**) and between differentially substituted phenyl rings (Table 2, compounds **5d**, **5i**, **5j**).

Although the size of the alkyl side chain of the nitrogen does not influence the viscosity sensitivity (all slope numbers are between 0.51 and 0.55) they do affect the brightness of the dye as shown by the y -intercept data (Table 2: **5b**=50, **5d**=85, **5k**=127, and **5m**=200). Replacement of the nitrile group by a methyl ester or phenyl sulfonyl motif resulted in increase of the emission quantum yield (Table 2, compounds **5c**, **5e**, **5f**). These results can be explained by considering the effect of these changes to the overall dipole moment of the probes. It is known that, upon excitation, the TICT probes assume a planar and dipolar quinoid structure (**B**), the stability of which is affected by the dipole moment and charge distribution (Fig. 4). Thus, changes in the molecular structure that stabilize the excited state lead to an increase of the fluorescence intensity. It should be noted that a similar increase of fluorescence has been observed with a series of dialkylaminobenzonitriles and has been explained based on the dipole moment.³³

An increase in the brightness is also observed when the phenyl group of **5d** or **5f** is functionalized with an additional methoxy substituent (rotor **5i** or **5h**, respectively). Similarly, the more electronically rich thiophenyl group of rotor **14** is brighter than **5d**.³⁴ These results suggest that increasing the electron density between the donor and acceptor units leads to an increase of fluorescence. This electronic effect can, however, be compromised by steric effects.³⁵ The steric congestion due to substitution at the periphery of the phenyl ring can destabilize the planar structure (**B**) of the excited state. Along these lines, compound **18** is among the least bright dyes despite the presence of the two electronically donating methoxy groups. Similar effects have been recorded in a series of methoxy-substituted stilbenes.^{35,36}

It is also interesting to compare the naphthyl compounds **7** and **11**. The presence of the donor and acceptor groups along the long axis of naphthalene of rotor **11** increases significantly the Stokes shift and intensity, as compared to **7**. This can be explained by considering that substituents along the long axis of naphthalene decrease significantly the lowest singlet excited state.³⁷ This results to an increase of the energy gap between that excited state and the TICT states rendering the compound more bright but less sensitive to environmental changes. On the other hand, substituents along the short axis of naphthalene, such as in rotor **7**, decrease the second lowest excited state and thus increase the coupling of this state with the TICT states.³⁷

Theoretical studies by Förster and Hoffmann³⁰ have predicted that the maximum viscosity sensitivity of a molecular rotor is 0.66 assuming that the deexcitation of this molecule takes place predominantly via intramolecular rotation. In solvents with the viscosity range used in our study, this prerequisite is met. In most cases the viscosity sensitivity of the molecular rotors was found to be between 0.4 and 0.6. It is interesting to observe that most chemical modifications that increase the fluorescence intensity result in a decrease of the viscosity sensitivity. In fact, compound **18**, one of the least bright dyes of this study, exhibits one of the highest sensitivity values. On the other hand, naphthalene-based rotor **11** is the brightest dye but has the smallest value of viscosity sensitivity. This suggests that a dye that exhibits low intensity at

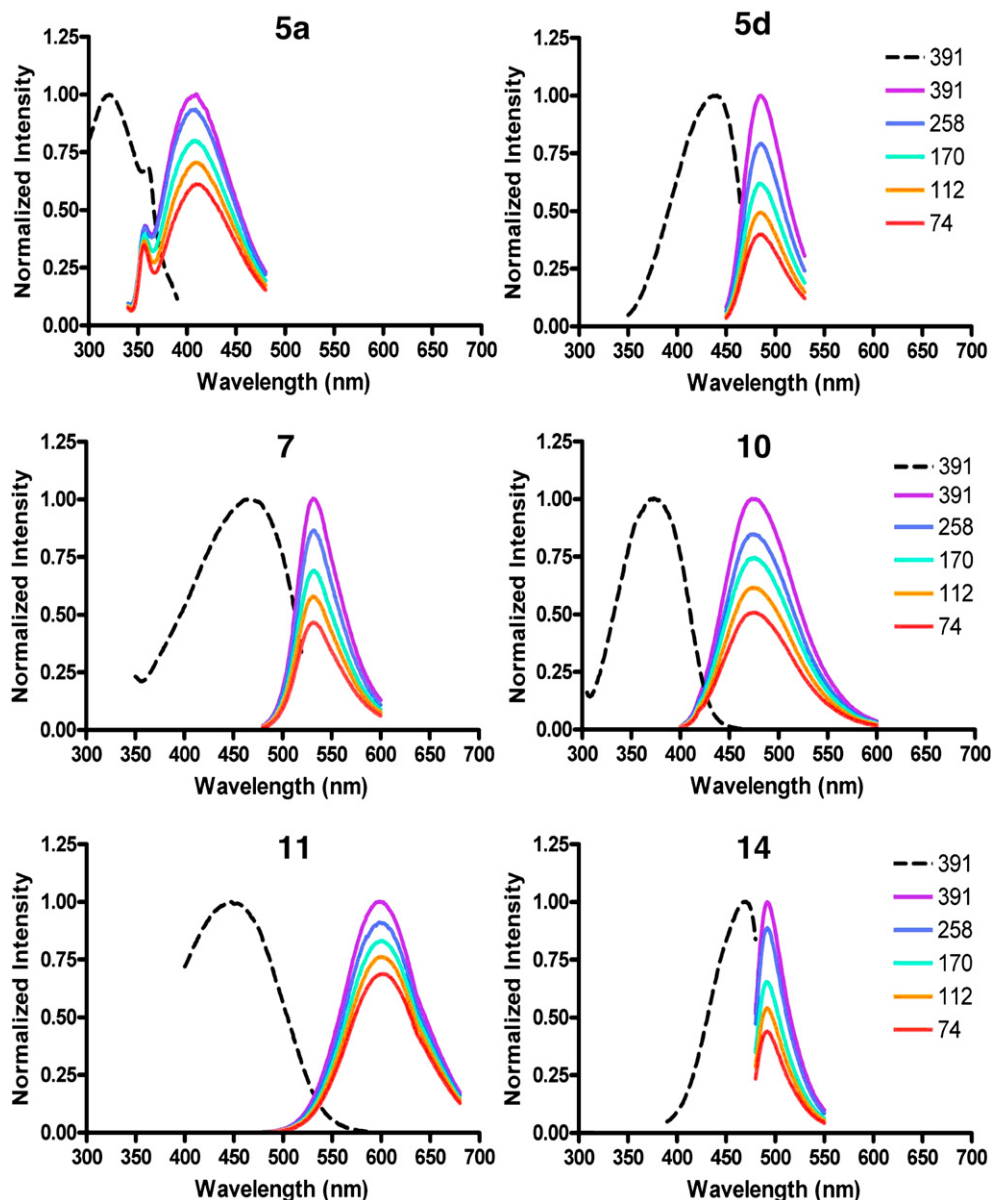


Figure 2. Normalized fluorescence excitation and emission spectra for compounds 5a, 5d, 7, 10, 11, and 14.

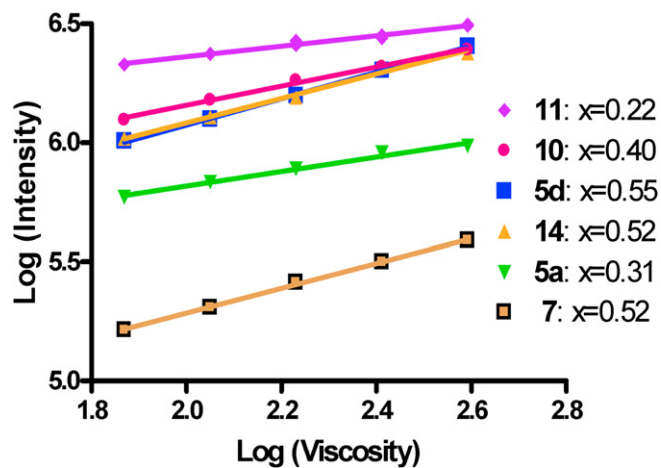


Figure 3. Emission intensities of rotors 5a, 5d, 7, 10, 11, and 14 in mixtures of ethylene glycol/glycerol (emission maxima in Table 2) drawn over the viscosity of the mixtures in a double-logarithmic scale.

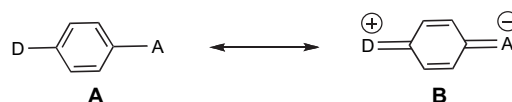


Figure 4. Mesomeric structures of a TICT probe. Upon photoexcitation, the ground-state structure (A) is converted to a dipolar quinoid structure (B).

a low viscosity can increase its viscosity related intensity faster, and thus have a higher sensitivity, as compared to a bright dye.

4. Conclusions

In this study we examined the effects of the chemical functionalities of molecular rotors to the fluorescence profile, brightness and viscosity sensitivity. The excitation and emission maxima for these compounds can be tuned by the extent of conjugation between the electron donor and electron acceptor groups. In addition, the brightness of these dyes can be tuned by modifying the

electron density between the electron donor and electron acceptor groups and by the presence of alkyl side chains on the donor group. Moreover, chemical changes that increase the brightness of a molecular rotor, lead to a decrease of its viscosity sensitivity. The understanding of the effect of the chemical structure to the fluorescence profile should help the rational design of molecular rotors that are optimized for a specific application.

5. Experimental section

5.1. General notes

6-Methoxy-2-naphthaldehyde **8** was purchased from Alfa Aesar. The rest of the reagents were obtained (Aldrich, Acros) at highest commercial quality and used without further purification except where noted. Air- and moisture-sensitive liquids and solutions were transferred via syringe or stainless steel cannula. Organic solutions were concentrated by rotary evaporation below 45 °C at approximately 20 mmHg. All non-aqueous reactions were carried out under anhydrous conditions. Yields refer to chromatographically and spectroscopically (¹H NMR, ¹³C NMR) homogeneous materials, unless otherwise stated. Reactions were monitored by thin-layer chromatography (TLC) carried out on 0.25 mm E. Merck silica gel plates (60F-254) and visualized under UV light and/or developed by dipping in solutions of 10% ethanolic phosphomolybdic acid (PMA) or *p*-anisaldehyde and applying heat. E. Merck silica gel (60, particle size 0.040–0.063 mm) was used for flash chromatography. Preparative thin-layer chromatography separations were carried out on 0.25 or 0.50 mm E. Merck silica gel plates (60F-254). NMR spectra were recorded on Varian Mercury 400 and/or Unity 500 MHz instruments and calibrated using the residual non-deuterated solvent as an internal reference. The following abbreviations were used to explain the multiplicities: s=singlet, d=doublet, t=triplet, q=quartet, m=multiplet, br=broad. High resolution mass spectra (HRMS) were recorded on a VG 7070 HS mass spectrometer under electron spray ionization (ESI) or electron impact (EI) conditions. Fluorescence spectroscopy data were recorded on a Jobin-Yvon Fluoromax-3 instrument.

5.2. General procedure for the preparation of molecular rotors

To a round bottom flask containing a solution of aldehyde (5.0 mmol) and methyl 2-cyanoacetate (5.5 mmol) in 20 mL of methanol was added 0.50 mmol of piperidine and the mixture was heated at 50 °C. The formation of the product was monitored by TLC and was completed within 8 h. Note that in certain cases the product precipitates out of the reaction mixture. The crude mixture was concentrated under reduced pressure and the product was collected by a vacuum filtration. Alternatively, the product was purified via flash chromatography (10–30% ethyl acetate in hexane).

5.2.1. (E)-Methyl 2-cyano-3-(4-methoxyphenyl)acrylate (5a). Yield 48%; yellow solid; ¹H NMR (400 MHz, CDCl₃) δ 8.19 (s, 1H), 8.01 (d, 2H, J=8.9 Hz), 7.00 (d, 2H, J=8.9 Hz), 3.92 (s, 3H), 3.90 (s, 3H); ¹³C NMR (100 MHz, CDCl₃) δ 163.8, 163.5, 154.6, 133.6, 124.1, 116.1, 114.7, 98.6, 55.5, 53.1; HRMS calcd for C₁₂H₁₁NO₃ (M+Na)⁺ 240.0631, found 240.0633.

5.2.2. (E)-Methyl 3-(4-aminophenyl)-2-cyanoacrylate (5b). Yield 87%; yellow solid; ¹H NMR (400 MHz, CDCl₃) δ 8.09 (s, 1H), 7.88 (d, 2H, J=8.7 Hz), 6.69 (d, 2H, J=8.7 Hz), 4.36 (s, 2H), 3.89 (s, 3H); ¹³C NMR (100 MHz, CDCl₃) δ 164.2, 154.8, 152.8, 134.1, 120.3, 117.1, 114.0,

93.7, 52.6; HRMS calcd for C₁₁H₁₀N₂O₂ (M+H)⁺ 203.0815, found 203.0822.

5.2.3. 2-(4-Aminobenzylidene)malononitrile (5c). Yield 65%; dark yellow solid; ¹H NMR (400 MHz, DMSO) δ 7.97 (s, 1H), 7.72 (d, 2H, J=8.8 Hz), 7.02 (s, 2H), 6.66 (d, 2H, J=8.8 Hz); ¹³C NMR (100 MHz, DMSO) δ 159.7, 156.7, 135.1, 119.6, 117.1, 116.3, 114.3, 68.5; HRMS calcd for C₁₀H₇N₃ (M)⁺ 169.0634, found 169.0636.

5.2.4. (E)-Methyl 2-cyano-3-(4-(dimethylamino)phenyl) acrylate (5d). Yield 89%; yellow solid; ¹H NMR (400 MHz, CDCl₃) δ 8.06 (s, 1H), 7.92 (d, 2H, J=9.0 Hz), 6.68 (d, 2H, J=9.1 Hz), 3.87 (s, 3H), 3.10 (s, 6H); ¹³C NMR (100 MHz, CDCl₃) δ 165.0, 155.0, 153.9, 134.3, 119.5, 117.8, 111.7, 93.6, 53.0, 40.2; HRMS calcd for C₁₃H₁₄N₂O₂ (M+H)⁺ 231.1128, found 231.1126.

5.2.5. 2-(4-Dimethylaminobenzylidene)malononitrile (5e). Yield 91%; orange solid; ¹H NMR (400 MHz, CDCl₃) δ 7.78 (d, 2H, J=8.8 Hz), 7.41 (s, 1H), 6.68 (d, 2H, J=8.9 Hz), 3.14 (s, 6H); ¹³C NMR (100 MHz, CDCl₃) δ 158.0, 154.1, 133.7, 119.1, 116.0, 114.9, 111.5, 71.3, 40.0; HRMS calcd for C₁₂H₁₁N₃ (M+H)⁺ 198.1026, found 198.1024.

5.2.6. (E)-3-(4-(Dimethylamino)phenyl)-2-(phenylsulfonyl) acrylonitrile (5f). Yield 92%; orange solid; ¹H NMR (400 MHz, CDCl₃) δ 7.99 (s, 1H), 7.97 (s, 2H), 7.81 (d, 2H, J=9.1 Hz), 7.62 (m, 1H), 7.55 (m, 2H), 6.65 (d, 2H, J=9.1 Hz), 3.10 (s, 6H); ¹³C NMR (100 MHz, CDCl₃) δ 154.0, 151.1, 139.6, 134.0, 133.7, 129.3, 127.9, 117.6, 115.0, 111.5, 104.6, 40.0; HRMS calcd for C₁₇H₁₆N₂O₂S (M+H)⁺ 313.1005, found 313.1004.

5.2.7. Dimethyl 2-(4-(dimethylamino)benzylidene)malonate (5g). Yield 17%; yellow solid; ¹H NMR (400 MHz, CDCl₃) δ 7.67 (s, 1H), 7.33 (d, 2H, J=8.9 Hz), 6.63 (d, 2H, J=9.0 Hz), 3.88 (s, 3H), 3.81 (s, 3H), 3.03 (s, 6H); ¹³C NMR (100 MHz, CDCl₃) δ 168.4, 165.3, 151.9, 143.5, 131.8, 119.8, 118.9, 111.5, 52.4, 52.2, 39.9; HRMS calcd for C₁₄H₁₇O₄N (M)⁺ 263.1155, found 263.1152.

5.2.8. (E)-3-(4-(Dimethylamino)-2-methoxyphenyl)-2-(phenylsulfonyl) acrylonitrile (5h). Yield 81%; yellow solid; ¹H NMR (400 MHz, CDCl₃) δ 8.51 (s, 1H), 8.12 (d, 1H, J=9.2 Hz), 7.97 (d, 2H, J=7.5 Hz), 7.60 (m, 1H), 7.53 (m, 2H), 6.26 (dd, 1H, J=2.1, 9.2 Hz), 5.98 (d, 1H, J=2.1 Hz), 3.89 (s, 3H), 3.11 (s, 6H); ¹³C NMR (100 MHz, CDCl₃) δ 162.1, 156.2, 144.8, 140.2, 133.4, 130.7, 129.2, 127.8, 115.8, 107.9, 105.3, 102.4, 92.6, 55.4, 40.2; HRMS calcd for C₁₈H₁₈N₂O₃S (M+H)⁺ 343.1111, found 343.1110.

5.2.9. (E)-Methyl 2-cyano-3-(4-(dimethylamino)-2-methoxyphenyl) acrylate (5i). Yield 89%; orange solid; ¹H NMR (400 MHz, CDCl₃) δ 8.62 (s, 1H), 8.36 (d, 1H, J=9.2 Hz), 6.31 (dd, 1H, J=2.4, 9.2 Hz), 6.00 (d, 1H, J=2.4 Hz), 3.87 (s, 3H), 3.85 (s, 3H), 3.09 (s, 6H); ¹³C NMR (100 MHz, CDCl₃) δ 165.5, 162.2, 155.9, 148.4, 131.2, 118.6, 109.6, 105.4, 93.1, 91.8, 55.6, 52.8, 40.4; HRMS calcd for C₁₄H₁₆N₂O₃ (M+H)⁺ 261.1234, found 261.1235.

5.2.10. (E)-Methyl 2-cyano-3-(4-(dimethylamino)-2-methylphenyl) acrylate (5j). Yield 86%; yellow solid; ¹H NMR (300 MHz, CDCl₃) δ 8.44 (s, 1H), 8.41 (s, 1H), 6.57 (dd, 1H, J=2.5, 9.1 Hz), 6.47 (d, 1H, J=2.3 Hz), 3.87 (s, 3H), 3.07 (s, 6H), 2.43 (s, 3H); ¹³C NMR (100 MHz, CDCl₃) δ 165.3, 153.8, 151.5, 144.0, 131.3, 118.4, 118.2, 113.1, 110.1, 93.5, 53.0, 44.4, 40.2, 20.8; HRMS calcd for C₁₄H₁₆N₂O₂ (M+H)⁺ 245.1285, found 245.1289.

5.2.11. (E)-Methyl 2-cyano-3-(4-diethylaminophenyl) acrylate (5k). Yield 67%; brown solid; ¹H NMR (400 MHz, CDCl₃) δ 8.01 (s, 1H), 7.88 (d, 2H, J=9.1 Hz), 6.64 (d, 2H, J=9.2 Hz), 3.84 (s, 3H), 3.42 (q, 4H, J=7.1 Hz), 1.19 (t, 6H, J=7.1 Hz); ¹³C NMR (100 MHz, CDCl₃)

δ 164.8, 154.4, 151.6, 134.4, 118.6, 117.7, 111.0, 92.4, 52.6, 44.7, 12.4; HRMS calcd for $C_{15}H_{18}N_2O_2$ (M+H)⁺ 259.1441, found 259.1430.

5.2.12. 4-(2,2-Bis(phenylsulfonyl)vinyl)-N,N-dimethylaniline (**5I**). Yield 2%; yellow solid; ¹H NMR (400 MHz, CDCl₃) δ 8.45 (s, 1H), 8.02 (t, 4H, *J*=7.5 Hz), 7.90 (d, 2H, *J*=9.0 Hz), 7.43–7.59 (m, 6H), 6.61 (d, 2H, *J*=9.0 Hz), 3.09 (s, 6H); ¹³C NMR (400 MHz, CDCl₃) δ 153.6, 151.5, 141.9, 141.7, 137.5, 133.3, 133.0, 128.9, 128.8, 128.7, 128.1, 127.2, 117.0, 112.2, 40.0; HRMS calcd for $C_{22}H_{21}NO_4S_2$ (M+H)⁺ 428.0985, found 428.0984.

5.2.13. (E)-Methyl 2-cyano-3-(4-(dibutylamino)phenyl)acrylate (**5m**). Yield 72%; orange solid; ¹H NMR (400 MHz, CDCl₃) δ 8.04 (s, 1H), 7.91 (d, 2H, *J*=9.1 Hz), 6.64 (d, 2H, *J*=9.2 Hz), 3.88 (s, 3H), 3.36 (m, 4H), 1.60 (m, 4H), 1.37 (m, 4H), 0.97 (t, 6H, *J*=7.3 Hz); ¹³C NMR (100 MHz, CDCl₃) δ 164.9, 154.4, 152.0, 134.3, 118.6, 117.8, 111.2, 92.4, 52.6, 50.8, 29.2, 20.1, 13.8; HRMS calcd for $C_{19}H_{26}N_2O_2$ (M+H)⁺ 315.2067, found 315.2056.

5.2.14. (E)-Methyl 2-cyano-3-(4-(dimethylamino)naphthalene-1-yl)acrylate (**7**). Yield 98%; yellow solid; ¹H NMR (400 MHz, CDCl₃) δ 9.07 (s, 1H), 8.51 (d, 1H, *J*=8.3 Hz), 8.20 (d, 1H, *J*=8.4 Hz), 8.11 (d, 1H, *J*=8.4 Hz), 7.61 (m, 1H), 7.55 (m, 1H), 7.06 (d, 1H, *J*=8.3 Hz), 3.96 (s, 3H), 3.05 (s, 6H); ¹³C NMR (100 MHz, CDCl₃) δ 164.1, 156.7, 151.9, 134.2, 130.2, 128.0, 127.6, 126.0, 125.5, 123.3, 121.2, 117.0, 112.7, 100.0, 53.4, 44.8; HRMS calcd for $C_{17}H_{16}N_2O_2$ (M+H)⁺ 281.1285, found 281.1287.

5.2.15. (E)-Methyl 2-cyano-3-(6-methoxynaphthalen-2-yl)acrylate (**10**). Yield 87%; yellow solid; ¹H NMR (400 MHz, CDCl₃) δ 8.37 (s, 1H), 8.32 (d, 1H, *J*=2.4 Hz), 8.18 (dd, 1H, *J*=1.8, 8.7 Hz), 7.85–7.79 (m, 2H), 7.21 (dd, 1H, *J*=2.5, 8.9 Hz), 7.16 (s, 1H), 3.97 (s, 3H), 3.95 (s, 3H); ¹³C NMR (400 MHz, CDCl₃) δ 163.5, 160.4, 155.3, 137.3, 134.3, 131.1, 128.1, 127.8, 126.8, 126.0, 120.2, 116.1, 105.9, 100.3, 55.5, 55.3; HRMS calcd for $C_{16}H_{13}NO_3$ (M+Na)⁺ 290.0788, found 290.0791.

5.2.16. (E)-Methyl 2-cyano-3-(6-piperidin-1-yl naphthalen-2-yl)acrylate (**11**). Yield 90%; orange solid; ¹H NMR (300 MHz, CDCl₃) δ 8.29 (s, 1H), 8.19 (s, 1H), 8.09 (dd, 1H, *J*=1.8, 8.8 Hz), 7.74 (d, 1H, *J*=9.2 Hz), 7.64 (d, 1H, *J*=8.8 Hz), 7.28 (dd, 1H, *J*=2.6, 9.3 Hz), 7.03 (d, 1H, *J*=2.2 Hz), 3.93 (s, 3H), 3.39 (t, 4H, *J*=5.1 Hz), 1.73–1.66 (m, 6H); ¹³C NMR (100 MHz, CDCl₃) δ 163.9, 155.5, 151.9, 137.7, 134.7, 130.6, 127.2, 126.4, 126.0, 125.6, 119.3, 116.6, 108.3, 98.3, 53.1, 49.3, 25.5, 24.3; HRMS calcd for $C_{20}H_{20}N_2O_2$ (M+H)⁺ 321.1598, found 321.1601.

5.2.17. (E)-Methyl 2-cyano-3-(5-(piperidin-1-yl)thiophen-2-yl)acrylate (**14**). Yield 90%; orange solid; ¹H NMR (400 MHz, CDCl₃) δ 7.95 (s, 1H), 7.38 (br s, 1H), 6.07 (d, 1H, *J*=4.6 Hz), 3.76 (s, 3H), 3.39 (br s, 4H), 1.64 (m, 6H); ¹³C NMR (100 MHz, CDCl₃) δ 169.2, 165.4, 146.1, 144.1, 119.4, 118.4, 104.8, 61.5, 51.1, 24.8, 23.3; HRMS calcd for $C_{14}H_{16}N_2O_2S$ (M+H)⁺ 277.1005, found 277.1006.

5.2.18. (E)-Methyl 2-cyano-3-(4-(diethylamino)-2,6-dimethoxyphenyl)acrylate (**18**). Yield 81%; yellow solid; ¹H NMR (300 MHz, CDCl₃) δ 8.47 (s, 1H), 5.72 (s, 2H), 3.86 (s, 6H), 3.84 (s, 3H), 3.41 (q, 4H, *J*=7.1 Hz) 1.22 (t, 6H, *J*=7.1 Hz); ¹³C NMR (100 MHz, CDCl₃) δ 166.5, 162.6, 153.9, 146.3, 118.0, 101.1, 95.4, 87.0, 55.0, 52.8, 45.2, 12.9; HRMS calcd for $C_{17}H_{22}N_2O_4$ (M+H)⁺ 319.1652, found 319.1657.

5.2.19. 6-(Piperidin-1-yl)-2-naphthaldehyde (**9**). To a 50 mL round bottom flask containing benzene (3 mL), HMPA (3 mL), and piperidine (1.65 mL, 16.7 mmol) was added via syringe, at 0 °C, *n*-BuLi (1.6 M in hexane, 10.4 mL, 16.7 mmol). After stirring for 15 min, the reaction mixture was treated with a solution of 6-methoxy-2-naphthaldehyde (390 mg, 2.09 mmol) in benzene/HMPA 1:1

(2 mL). The reaction mixture was warmed to room temperature, left stirring for 12 h and then it was poured into cold 5% aqueous NaCl (30 mL). The mixture was extracted with diethyl ether (3×20 mL), dried over MgSO₄, and concentrated. The product was purified via flash chromatography (20% EtOAc in hexanes) to give compound **9**. Compound **9**: 35% yield, yellow solid; ¹H NMR (300 MHz, CDCl₃) δ 10.02 (s, 1H), 8.14 (s, 1H), 7.88–7.73 (m, 2H), 7.67 (d, 1H, *J*=8.6 Hz), 7.32 (dd, 1H, *J*=2.5, 9.1 Hz), 7.08 (d, 1H, *J*=2.4 Hz), 3.42–3.32 (m, 4H), 1.85–1.57 (m, 6H); ¹³C NMR (100 MHz, CDCl₃) δ 192.2, 152.2, 138.8, 134.7, 131.6, 130.7, 127.5, 126.5, 123.6, 119.7, 109.0, 49.8, 25.8, 24.6; HRMS calcd for $C_{16}H_{17}NO$ (M+H)⁺ 240.1383, found 240.1387.

5.2.20. 5-(Piperidin-1-yl)thiophene-2-carbaldehyde (**13**). A 200 mL round bottom flask containing 5-bromothiophene-2-carbaldehyde (7.62 g, 400 mmol), piperidine (3.40 g, 400 mmol), toluene (30 mL), and *p*-toluene sulfonic acid (0.69 g, 40 mmol) was refluxed for 24 h. The crude mixture was concentrated and the residue was subjected to flash chromatography using dichloromethane/ethyl ether/hexane: 1:1:8 to give aldehyde **13**. This compound was further crystallized from dichloromethane/hexane. Compound **13**: 72% yield, dark blue solid; ¹H NMR (400 MHz, CDCl₃) δ 9.51 (s, 1H), 7.47 (d, 1H, *J*=4.4 Hz), 6.06 (d, 1H, *J*=4.4 Hz), 3.35 (t, 4H, *J*=4.7, 11.0 Hz), 1.73–1.65 (m, 6H); ¹³C NMR (100 MHz, CDCl₃) δ 180.4, 168.6, 140.6, 126.6, 104.2, 51.1, 25.1, 23.7; HRMS calcd for $C_{10}H_{13}NOS$ (M+H)⁺ 196.0791, found 196.0792.

5.2.21. 4-(Diethylamino)-2,6-dimethoxybenzaldehyde (**17**). To a 10 mL round bottom flask containing *N,N*-diethyl-3,5-dimethoxyaniline²⁷ (99.7 mg, 0.48 mmol) and DMF (150 μ L, 0.96 mmol) in DCM (2 mL) was added dropwise POCl₃ (82.2 mg, 0.05 mL, 0.54 mmol) and the reaction mixture was stirred at 25 °C for 5 h. Sodium hydroxide (2 M, 15 drops) was then added until the solution became neutral causing the color to change to dark blue and the mixture was stirred at 0 °C for 3 h. The mixture was extracted with ether (2×10 mL) and the organic extracts were dried over MgSO₄ and concentrated. The product was purified by flash column chromatography (50% EtOAc in hexanes). Compound **17**: 65% yield, white crystals; ¹H NMR (400 MHz, CDCl₃) 10.17 (s, 1H), 5.68 (s, 2H), 3.82 (s, 6H), 3.38 (q, 4H, *J*=7.1 Hz), 1.19 (t, 6H, *J*=7.1 Hz); ¹³C NMR (75 MHz, CDCl₃) 186.6, 164.6, 153.9, 105.1, 86.8, 55.9, 55.8, 45.0, 12.9; HRMS calcd for $C_{13}H_{19}NO_3$ (M)⁺ 237.1359, found 237.1356.

5.3. General procedure for the determination of spectral properties

Each viscosity sample was mixed according to column A in Table 3 shown below. The glycerol (Gly) was heated to ensure more exact measuring during pipetting. The pre-stained ethylene glycol (EG) for each sample contained 100 μ M of dye resulting in a final

Table 3
Preparation of an ethylene glycol–glycerol viscosity gradient.

A	B	C
Pre-stained EG/EG/Gly volumes (mL)	Viscosity (mPa s)	log viscosity
0.5:0.5:4.0	391.4	2.593
0.5:1.0:3.5	258.1	2.412
0.5:1.5:3.0	170.2	2.231
0.5:2.0:2.5	112.2	2.050
0.5:2.5:2.0	74.0	1.869

concentration of 10 μ M for each sample. All samples were placed on rotating mixer for 1 h before pouring into cuvettes for scanning. Preliminary fluorescent scanning was done on each dye dissolved in 391.4 mPa s viscosity solvent to determine optimal excitation and peak emission and slit settings for each molecular rotor

derivative. All fluorescent scanning was done with the temperature-controlled turret set at room temperature (22 ± 0.8 °C); each sample was inserted in the turret and allowed to equilibrate for 10 min before testing. For each solvent the fluorescent emission in an 11 nm range was averaged and the logarithm of the average peak intensity was plotted against the logarithm of the viscosity. The slope was obtained for each molecular rotor derivative by linear regression (Graphpad Prism 4.01, San Diego, CA). The exponent x of each viscosity gradient was used to evaluate viscosity sensitivity, with a higher value of the exponent x indicating higher sensitivity. R^2 values indicate the linear regression of the log-transformed data (intensity over viscosity). When two or more similar experiments were performed the lowest value of R^2 is given (Table 2).

Acknowledgements

Financial support by the NIH (1R21RR025358) and the NSF (CMMI-0652476) is gratefully acknowledged. We thank the National Science Foundation for instrumentation grants CHE-9709183 and CHE-0741968. We also thank Drs. A. Mrse and Dr. Y. Su for NMR spectroscopic and mass spectrometric assistance, respectively.

Supplementary data

^1H and ^{13}C NMR spectra of compounds **5a–5m**, **7–11**, **13**, **14**, and **16–18**. Supplementary data associated with this article can be found in the online version, at doi:10.1016/j.tet.2010.01.093.

References and notes

- For selected reviews and monographs see: (a) Luby-Phelps, K. *Intern. Rev. Cytol.* **2000**, *192*, 189–221; (b) *Molecular and Cellular Aspects of Basement Membranes*; Rohrbach, D. H., Timpl, R., Eds.; Academic: San Diego, CA, 1993; (c) *The Membranes of Cells*; Yeagle, P. L., Ed.; Academic: San Diego, CA, 1993; (d) *Membrane Abnormalities in Sickle Cell Disease and in Other Red Blood Cell Disorders*; Ohnishi, S. T., Ohnishi, T., Eds.; CRC: Boca Raton, FL, 1994.
- For representative reviews see: (a) Reinhart, W. H. *Biorheology* **2001**, *38*, 203–212; (b) Moriarty, P. M.; Gibson, C. A. *Cardiovasc. Rev. Rep.* **2003**, *24*, 321–325; (c) Uchimura, I.; Numano, F. *Diabetes Frontier* **1997**, *8*, 33–37; (d) Simon, A.; Gariepy, J.; Chironi, G.; Megnien, J.-L.; Levenson, J. J. *Hypertens.* **2002**, *20*, 159–169.
- Oppenheimer, N.; Diamant, H. *Biophys. J.* **2009**, *96*, 3041–3049; Owen, D. M.; Williamson, D.; Rentero, C.; Gaus, K. *Traffic* **2009**, *10*, 962–971; Frick, M.; Schmidt, K.; Nichols, B. J. *Curr. Biol.* **2007**, *17*, 462–467.
- Luneva, O. G.; Brazhe, N. A.; Maksimova, N. V.; Rodnenkov, O. V.; Parsina, E. Y.; Bryzgalova, N. Y.; Maksimov, G. V.; Rubin, A. B.; Orlov, S. N.; Chazov, E. I. *Pathophysiology* **2007**, *14*, 41–46.
- Goodwin, J. S.; Drake, K. R.; Remment, C. L.; Kenworthy, A. K. *Biophys. J.* **2005**, *89*, 1398–1410; Dibner, M. D.; Ireland, K. A.; Koerner, L. A.; Dexter, D. L. *Cancer Res.* **1985**, *45*, 4998–5003.
- Aleardi, A. M.; Benard, G.; Augereau, O.; Malgat, M.; Talbot, J. C.; Mazat, J. P.; Letellier, T.; Dachary-Prigent, J.; Solaini, G. C.; Rossignol, R. J. *Bioenerg. Biomembr.* **2005**, *37*, 207–225; Hou, X.; Richardson, S. J.; Aguilar, M.-I.; Small, D. H. *Biochemistry* **2005**, *44*, 11618–11627.
- Ahn, J. H.; Kim, T. Y.; Kim, Y.-J.; Han, M. W.; Yoon, T. H.; Chung, J. W. *Diabet. Med.* **2006**, *23*, 1339–1343; Salazar Vasquez, B. Y.; Salazar Vasquez, M. A.; Venzor, V. C.; Negrete, A. C.; Cabrales, P.; Diaz, J. S.; Intaglietta, M. *Clin. Hemorheol. Microcirc.* **2008**, *38*, 67–74.
- Kearney-Schwartz, A.; Virion, J. M.; Stoltz, J.-F.; Drouin, P.; Zannad, F. *Fund. Clin. Pharmacol.* **2007**, *21*, 387–396.
- Velcheva, I.; Antonova, N.; Dimitrova, V.; Dimitrov, N.; Ivanov, I. *Clin. Hemorheol. Microcirc.* **2006**, *35*, 155–157.
- Bosman, G. J. C. G. M.; Bartholomeus, I. G. P.; de Grip, W. J. *Gerontology* **1991**, *37*, 95–112.
- International Committee for Standardization in Haematology. *J. Clin. Pathol.* **1984**, *37*, 1147–1152.
- Wang, S.; Boss, A. H.; Kensey, K. R.; Rosenson, R. S. *Clin. Chim. Acta* **2003**, *332*, 79–82.
- Lakowicz, J. R. *Principles of Fluorescence Spectroscopy*; KLUWER ACADEMIC/PLENUM: New York, NY, 1999.
- Shinitzky, M.; Barenholz, Y. *Biochim. Biophys. Acta* **1978**, *515*, 367–394.
- (a) Axelrod, D.; Koppel, D. E.; Schlessinger, J.; Elson, E.; Webb, W. W. *Biophys. J.* **1976**, *16*, 1055–1069; (b) Soumpasis, D. M. *Biophys. J.* **1983**, *41*, 95–97; (c) Swaminathan, R.; Bicknese, S.; Periasamy, N.; Verkman, A. S. *Biophys. J.* **1996**, *71*, 1140–1151.
- Blonk, J. C. G.; Don, A.; van Aalst, H.; Birmingham, J. J. *J. Microsc.* **1993**, *169*, 363–374.
- (a) Haidekker, M. A.; Theodorakis, E. A. *Org. Biomol. Chem.* **2007**, *5*, 1669–1678; (b) Demchenko, P.; Mely, Y.; Duportail, G.; Klymchenko, A. S. *Biophys. J.* **2009**, *96*, 3461–3470.
- Grabowski, Z. R.; Rotkiewicz, K.; Rettig, W. *Chem. Rev.* **2003**, *103*, 3899–4031.
- (a) Loutfy, R. O. *Pure Appl. Chem.* **1986**, *58*, 1239–1248; (b) Levitt, J. A.; Kuimova, M. K.; Yahioglu, G.; Chung, P.-H.; Suhling, K.; Phillips, D. J. *Phys. Chem. C* **2009**, *113*, 11634–11642.
- Haidekker, M. A.; L'Heureux, N.; Frangos, J. A. *Am. J. Physiol. Heart Circ. Physiol.* **2000**, *278*, H1401–H1406.
- Haidekker, M. A.; Tsai, A. G.; Brady, T.; Stevens, H. Y.; Frangos, J. A.; Theodorakis, E. A.; Intaglietta, M. *Am. J. Physiol. Heart Circ. Physiol.* **2002**, *282*, H1609–H1614.
- (a) Loutfy, R. O.; Law, K. Y. J. *Phys. Chem.* **1980**, *84*, 2803–2808; (b) Haidekker, M. A.; Brady, T. P.; Lichlyter, D.; Theodorakis, E. A. *Bioorg. Chem.* **2005**, *33*, 415–425.
- (a) Haidekker, M. A.; Akers, W.; Lichlyter, D.; Brady, T. P.; Theodorakis, E. A. *Sens. Lett.* **2005**, *3*, 42–48; (b) Haidekker, M. A.; Brady, T. P.; Lichlyter, D.; Theodorakis, E. A. *J. Am. Chem. Soc.* **2006**, *128*, 398–399; (c) Fischer, D.; Theodorakis, E. A.; Haidekker, M. A. *Nat. Protoc.* **2007**, *2*, 227–236; (d) Nipper, M. E.; Majd, S.; Mayer, M.; Lee, J.; Theodorakis, E. A.; Haidekker, M. A. *Biochim. Biophys. Acta Biomembr.* **2008**, *1778*, 1148–1153.
- Chen, X.-X.; Zhao, Z.; Liu, Y.; Lu, P.; Wang, Y.-G. *Chem. Lett.* **2008**, *37*, 570–571.
- Guo, H.-M.; Tanaka, F. J. *Org. Chem.* **2009**, *74*, 2417–2424.
- Wuerthner, F.; Yao, S.; Schilling, J.; Wortmann, R.; Redi-Abshiro, M.; Mecher, E.; Gallego-Gomez, F.; Meerholz, K. J. *Am. Chem. Soc.* **2001**, *123*, 2810–2824.
- Razzuk, A.; Biehl, E. R. J. *Org. Chem.* **1987**, *52*, 2619–2622.
- Haidekker, M. A.; Ling, T.; Anglo, M.; Stevens, H. Y.; Frangos, J. A.; Theodorakis, E. A. *Chem. Biol.* **2001**, *8*, 123–131.
- Law, K. Y. *Chem. Phys. Lett.* **1980**, *75*, 545–549.
- Förster, Th.; Hoffmann, G. Z. *Phys. Chem.* **1971**, *75*, 63–76.
- DiCesare, N.; Lakowicz, J. R. J. *Phys. Chem. A* **2001**, *105*, 6834–6840.
- (a) Minakata, S.; Moriwaki, S.; Inada, H.; Komatsu, M.; Kajii, H.; Ohmori, Y.; Tsumura, M.; Namura, K. *Chem. Lett.* **2007**, *36*, 1014–1015; (b) Duan, L.; Xu, Y.; Qian, X.; Zhang, Y.; Liu, Y. *Tetrahedron Lett.* **2009**, *50*, 22–25.
- (a) Schuddeboom, W.; Jonker, S. A.; Warman, J. M.; Leinhos, U.; Kuehnle, W.; Zachariasse, K. A. J. *Phys. Chem.* **1992**, *96*, 10809–10819; (b) Il'ichev, Y. V.; Kuehnle, W.; Zachariasse, K. A. J. *Phys. Chem.* **1998**, *102*, 5670–5680.
- Yang, X.; Jiang, X.; Zhao, C.; Chen, R.; Qin, P.; Sun, L. *Tetrahedron Lett.* **2006**, *47*, 4961–4964.
- Shinohara, Y.; Arai, T. *Bull. Chem. Soc. Jpn.* **2008**, *81*, 1500–1504.
- (a) Roberts, J. C.; Pincock, J. A. J. *Org. Chem.* **2006**, *71*, 1480–1492; (b) Hayakawa, J.; Ikegami, M.; Mizutani, T.; Wahadoszamen, Md.; Monotake, A.; Nishimura, Y.; Arai, T. *J. Phys. Chem. A* **2006**, *110*, 12566–12571.
- Zachariasse, K. A.; Grobys, M.; von der Haar, Th.; Hebecker, A.; Il'ichev, Y. V.; Jiang, Y.-B.; Morawski, O.; Kuehnle, W. J. *Photochem. Photobiol., A: Chem.* **1996**, *102*, 59–70.